

## Band-to-acceptor transitions in the low-temperature-luminescence spectrum of Li-doped *p*-type ZnSe grown by molecular-beam epitaxy

Y. Zhang and B. J. Skromme

*Department of Electrical Engineering and Center for Solid State Electronics Research, Arizona State University, Tempe, Arizona 85287-5706*

H. Cheng

*3M Company, 201-1N-35, 3M Center, St. Paul, Minnesota 55144*

(Received 17 August 1992)

Photoluminescence (PL) and magnetospectroscopy (in magnetic fields up to 12 T) have been used to characterize the properties of Li-doped *p*-type heteroepitaxial ZnSe on GaAs grown by molecular-beam epitaxy (MBE). A conduction-band-to-acceptor ( $e-A^0$ ) peak at 2.706 eV has been observed and identified in low-temperature (1.7 K), low-excitation-level PL measurements, in addition to the more commonly reported donor-to-acceptor ( $D^0-A^0$ ) pair recombination peak at about 2.692 eV. The  $e^0-A^0$  peak appears to occur at low temperature only in *p*-type-doped material, which may explain why it has not previously been detected in ZnSe below about 25 K. PL measurements as a function of temperature, excitation intensity, and magnetic field have been performed to confirm and study the nature of the peak. The  $e-A^0$  peak shifts and broadens linearly with increasing temperature as expected, but does not show strong excitation intensity-dependent shifts or quench at high temperatures as the  $D^0-A^0$  peak does. The  $e-A^0$  peak becomes narrower and shifts linearly to higher energy in applied magnetic fields, reflecting the expected behavior of the lowest-energy Landau level in the conduction band. A light-hole binding energy of  $114.1 \pm 0.4$  meV in strained material is obtained from the intercept of a linear fit to the temperature-dependent  $e-A^0$  peak positions, which corresponds to  $114.4 \pm 0.4$  meV in unstrained material. The inapplicability of a linear Haynes's-rule-type of relationship to shallow acceptors in ZnSe is emphasized. An anomalous initial quenching of the  $e-A^0$  peak intensity is observed as the temperature is raised, followed by the more normal increase due to the thermal ionization of the donors. This observation is modeled in terms of the temperature dependence of the competing (nonradiative, etc.) recombination rates. From the position of the  $e-A^0$  peak as a function of magnetic field, we obtain an electron effective mass  $m_e^* = 0.17$ , neglecting spin splittings, which were not well resolved. In previous measurements of these samples, the  $e-A^0$  peak was tentatively identified as the *R*-band, which has been associated with transitions between preferentially paired interstitial Li donors and substitutional Li acceptors on Zn sites. Based on the present results, we show that, in fact, no direct evidence exists in the PL spectrum for the presence of interstitial Li donors in this MBE material, which has important implications when attempting to explain the present limitations on *p*-type-doping levels achievable with Li. The possibility of observing  $e-A^0$  peaks at low temperature should be considered in future analyses of PL spectra of *p*-type-doped ZnSe, to avoid similar errors in interpretation. The occurrence of the  $e-A^0$  peak as a function of growth temperature and Li doping concentration is discussed. We describe and model the splitting of the Li acceptor-bound exciton into a doublet in the strained material. Finally, we discuss the observation of an excited-state-donor-to-acceptor peak involving Li acceptors, and the observation of discrete donor-acceptor pair lines involving Li.

### I. INTRODUCTION

Zinc selenide is of considerable interest for blue-light-emitting devices, due to its wide and direct band gap ( $\sim 2.67$  eV at room temperature, which is in the blue portion of the visible spectrum) and zinc-blende structure with reasonable lattice match to GaAs (0.27%). However, the difficulty in achieving reliable *p*-type doping in ZnSe has hindered applications of this material for three decades, since only *n*-type ZnSe is easily obtained. Alkali metals, such as Li and Na, acting as substitutional acceptors on the Zn site have been used to dope the material and have been studied extensively.<sup>1-11</sup> In recent years, Li

doping has been employed in high-quality material grown on GaAs substrates by molecular-beam epitaxy (MBE). The same photoluminescence (PL) features previously observed in bulk material have been detected in Li-doped MBE material, and moderate success ( $\sim 10^{17}$  cm<sup>-3</sup> hole concentration) has been achieved.<sup>12-22</sup> However, important questions remain, such as the fundamental reason for the limited carrier concentrations that have been achieved to date, and the possible role of interstitial Li donors in compensating the material and causing doping instabilities in applied electric fields.<sup>14,16,17,23</sup>

In this paper, low-temperature PL has been employed to characterize Li-doped *p*-type ZnSe grown by MBE. A

new peak involving band-to-acceptor ( $e-A^0$ ) transitions has been observed at 1.7 K. This peak, which has never previously been identified to our knowledge at temperatures below about 25 K in either bulk or heteroepitaxial ZnSe, varies in intensity with growth conditions and dominates the whole spectrum in the most heavily doped sample. Variable-temperature and excitation intensity PL measurements have been used to confirm the nature of the peak. Magnetoluminescence measurements have also been performed to verify the assignment and to determine the electron effective mass. The position of the  $e-A^0$  peak is found to be very useful in directly determining the binding energy of the Li acceptor level, since the line shape is found not to be strongly affected by phonon coupling, in contrast to previous assertions.<sup>1</sup> The presence of this peak in low-temperature PL spectra is apparently a unique characteristic of at least some  $p$ -doped material, since it has never been detected in  $n$ -type samples. As we will show, it is extremely important to recognize the possible existence of this type of peak in  $p$ -ZnSe doped with any acceptor impurity, since failure to recognize it can lead to incorrect assignments and faulty conclusions concerning the behavior of the dopants. We note that  $e-A^0$  peaks are well known to occur at low temperature in ZnTe,<sup>24</sup> which is normally  $p$  type. Thus, it does not seem too surprising that they can be observed in ZnSe, now that  $p$ -type doping has become possible.

In addition to the ( $e-A^0$ ) peak, we discuss the observation of another peak involving excited state donor-to-acceptor ( $D_{n=2}^0-A^0$ ) transitions, similar to that previously observed in GaAs and InP.<sup>25</sup> The peak can only be resolved at high magnetic fields, where the  $e-A^0$  peak is narrowed by the field. At zero field it appears as unresolved broadening on the low-energy side of the  $e-A^0$  peak. Finally, we discuss the observation of discrete donor-acceptor pair lines involving Li, the splitting pattern of the Li-acceptor-bound-exciton peaks in the strained heteroepitaxial material, and local phonon modes related to Li.

## II. EXPERIMENT

All samples were grown in a Perkin-Elmer model 430 dual chamber MBE system. High-purity elemental Zn, Se, and Li sources were used to grow and dope the samples. Details of the MBE growth of the Li-doped samples have been described in Ref. 15. Results from secondary-ion-mass-spectroscopy (SIMS), capacitance-voltage ( $C-V$ ), and preliminary PL measurements for these samples have been published elsewhere.<sup>12-16</sup> In this work, the PL measurements were performed using cw excitation either by blue light at 2.816 or 2.836 eV from a dye laser with Stilbene 3 dye, or by UV light at 3.53 eV from an Ar<sup>+</sup> gas laser. A Janis Superveritemp optical cryostat and a 12-T superconducting solenoid in a similar cryostat were used for PL and magnetospectroscopy, respectively. Both Faraday and Voigt configurations were used in the magnetoluminescence measurements. The samples were freely suspended in flowing superfluid or gaseous He. Excitation powers of 1 mW or less were used at temperatures above 4 K, to avoid sample heating by the laser. A

1.0-m double monochromator with 1800 g/mm gratings, a cooled GaAs photomultiplier tube, and photon counting were employed. The spectra are corrected when necessary for the response of the measurement system. Further details of the apparatus have been given elsewhere.<sup>26</sup>

## III. RESULTS AND DISCUSSION

### A. Band-to-acceptor peak $e-A^0$ in Li-doped ZnSe

Variable-temperature PL spectra of the donor-acceptor pair region under low excitation for a sample with a total Li concentration of  $7 \times 10^{16} \text{ cm}^{-3}$  as determined by SIMS are shown in Fig. 1. In the low temperature (1.7 K) spectrum, we observe two LO- and three LO-phonon replicas of the Cu-bound exciton ( $I_1^D$ ) (Ref. 27) at 2.7164 and 2.6852 eV, and two no-phonon peaks at 2.706 and 2.690 eV, respectively. The lower-energy peak at 2.690 eV was observed and assigned as a donor-to-acceptor  $D^0-A^0$  peak in previous work.<sup>12,14-16</sup> Photoluminescence spectra recorded with variable excitation level (not shown) show that the position of this peak shifts to higher energy and the linewidth becomes broader with increasing excitation level, as the recombination shifts to closer pairs with shorter lifetimes and larger Coulomb interaction. This result clearly indicates that the peak is  $D^0-A^0$  in origin. The variable-temperature PL spectra in Fig. 1 fur-

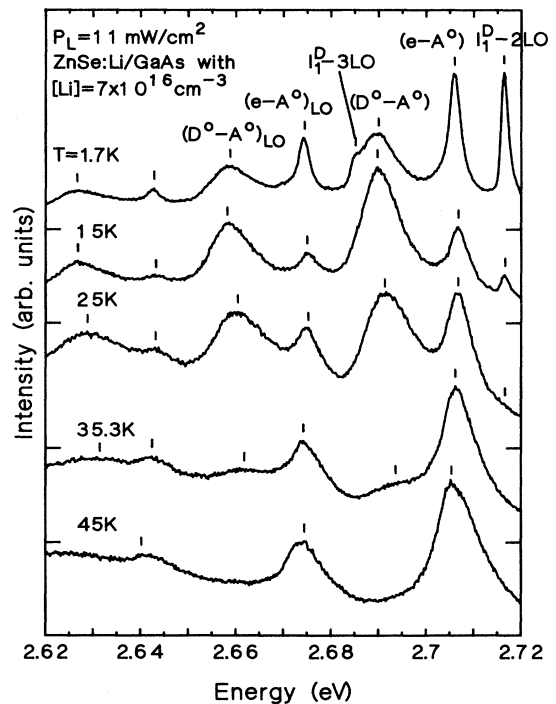


FIG. 1. PL spectra of the  $D^0-A^0$  pair region as a function of temperature under low-level UV excitation for a 2.9- $\mu\text{m}$ -thick ZnSe:Li/GaAs sample with a total Li concentration of  $7 \times 10^{16} \text{ cm}^{-3}$  and  $|N_A - N_D| = 2 \times 10^{16} \text{ cm}^{-3}$ . The instrumental resolution is 1 meV or better.

ther confirm this conclusion. As the temperature increases, the  $D^0-A^0$  peak quenches and disappears completely at around 45 K, due to thermal ionization of the donors into the conduction band at high temperature. This behavior is exactly that expected for a  $D^0-A^0$  peak. Moreover, the  $D^0-A^0$  peak shifts to higher energy as temperature increases, in the opposite direction to the shift of the band gap. Similar behavior was found by Dean and Merz.<sup>1</sup> This behavior can be understood as due to increasing competition from other radiative and nonradiative transitions, which compete more effectively with more distant donor-acceptor pairs having longer radiative lifetimes. Strong competition forces the recombination to shift to closer pairs with greater wave-function overlap and shorter lifetimes,<sup>28</sup> which produce higher-energy photons due to their enhanced Coulomb interaction.

In earlier studies, the higher-energy peak at 2.706 eV was tentatively assigned as the  $R$  band,<sup>11,16</sup> which is believed to involve  $D^0-A^0$  transitions between preferentially paired interstitial Li donors and substitutional Li acceptors on Zn sites. However, we see from Fig. 1 that this peak exhibits very different behavior from the  $D^0-A^0$  peak. The variable-temperature data show that this peak initially quenches with respect to the  $D^0-A^0$  peak as the temperature is raised. An explanation of this anomalous quenching will be given in Sec. III B by considering the temperature dependence of the competing nonradiative and other types of recombination. However, after this anomalous initial quenching, the peak becomes stronger and broader with increasing temperature and dominates the whole spectrum at high temperature, as shown in Fig. 1. The growth of the peak parallels the quenching of the  $D^0-A^0$  peak. This observation suggests that the peak is  $e-A^0$  in origin, since the thermal ionization of the donors should enhance its strength.

Photoluminescence spectra recorded as a function of excitation level (not shown) show that the 2.706-eV peak becomes stronger relative to the  $D^0-A^0$  peak at higher excitation, and does not appreciably shift in energy in the way that a  $D^0-A^0$  transition would be expected to do. This behavior is also consistent with the  $e-A^0$  assignment, since the  $D^0-A^0$  peak intensity is expected to saturate at high excitation once all of the available donors and acceptors have been neutralized. On the other hand, the concentration of electrons in the conduction band can be increased without limit, increasing the intensity of the  $e-A^0$  peak. The  $e-A^0$  peak position is expected to shift only if the electron temperature rises significantly. Based on this evidence, we conclude that the peak at 2.706 eV is a band-to-acceptor transition involving the substitutional Li acceptors. The peak is significantly narrower than all previously reported  $e-A^0$  peaks in ZnSe,<sup>1,3,5,29,30</sup> due to the lower temperature at which it is observable in the present material [the full width at half maximum (FWHM) of the peak is theoretically  $1.8k_B T$ , where  $k_B$  is Boltzmann's constant]. The magnetic-field dependence described in Sec. III D further confirms our identification.

Using parabolic curve fitting to the shift of the Li-acceptor-bound-exciton peak with temperature, we find

that the ZnSe band gap  $E_g(T)$  decreases with temperature in the range from 0 to 45 K according to

$$E_g(T) - E_g(0) = -1.3162 \times 10^{-6} T^2, \quad (1)$$

where  $E_g$  is in eV and  $T$  is in K. The actual  $e-A^0$  peak positions in Fig. 1, as well as corresponding values corrected using Eq. (1) for the shift of the band gap as a function of temperature, are plotted in Fig. 2. Neglecting any phonon broadening or strain splitting or broadening, the line shape of an  $e-A^0$  peak is given by<sup>31</sup>

$$I(\hbar\omega) = CE(E - E_g)^{1/2} \exp[-(E - E_g - E_A)/k_B T_e], \quad (2)$$

where  $E = \hbar\omega$  is the photon energy,  $C$  is approximately a constant,  $E_A$  is the acceptor binding energy,  $k_B$  is Boltzmann's constant, and  $T_e$  is the electron temperature. Neglecting the slowly varying  $E$  term, we find the peak position  $\hbar\omega_L(T)$  to be

$$\hbar\omega_L(T) = E_g(T) - E_A + k_B T_e / 2, \quad (3)$$

where  $T$  is the lattice temperature. This expression shows a linear variation of corrected peak position with electron temperature, where the slope and the intercept are given by  $k_B/2$  and  $E_g(T) - E_A$ , respectively. In general, the electron temperature may exceed the lattice temperature due to the photoexcitation, but usually approaches the lattice temperature at high lattice temperature.<sup>32</sup> However, a linear fit to the peak positions corrected for the temperature variation of  $E_g$  in Fig. 2, without assuming any increase in  $T_e$  over  $T$ , gives a very good fit with an intercept of 2.7061 eV and a slope of  $5.13 \times 10^{-5}$  eV/K. Therefore, we ignore electron heating and find that the slope agrees reasonably well with the theoretical value of  $k_B/2 = 4.32 \times 10^{-5}$  eV/K.

Comparing with bulk material, we find that the light-hole free-exciton peak is shifted 3.8 meV to lower energy due to biaxial tensile strain resulting from thermal mismatch with the GaAs substrate.<sup>33-35</sup> The same amount of shift is expected for the light-hole band gap, assuming that the binding energy of the free exciton,

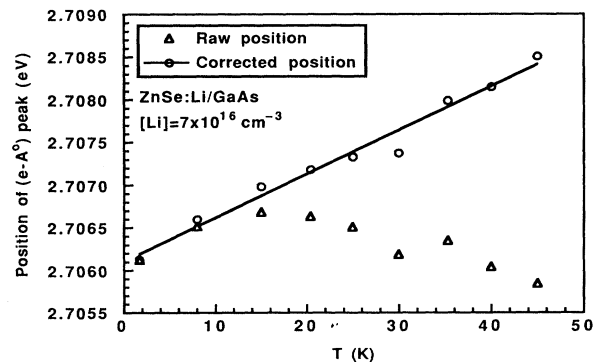


FIG. 2. Position of the  $e-A^0$  peak as a function of sample temperature for the sample of Fig. 1 (triangles), together with corresponding values corrected for the temperature-dependent shift in the band gap using Eq. (1) (circles). The solid line is a linear fit to the corrected data points, as described in the text.

which is mainly determined by the effective mass of the electron, is unchanged. Therefore, the light-hole band gap in this material is about 2.8180 eV, assuming  $E_g = 2.8218$  eV in unstrained material.<sup>36</sup> If we assume that the observed  $e-A^0$  peaks involve the ground-state (light-hole) acceptor levels, the 2.7061-eV intercept of the fit in Fig. 2 would imply an acceptor binding energy  $E_A = 111.9$  meV for light holes in the strained material. (An identical value is obtained by averaging the intercepts for four different samples, with an error of  $\pm 0.4$  meV.)

However, we believe that the peak we have observed in nearly all cases actually corresponds to the heavy-hole acceptor level. This conclusion follows from the fact that transitions involving the heavy-hole level have three times larger oscillator strength, as shown previously, for example, in magneto-optical studies of the  $e-A^0$  peak.<sup>24,37,38</sup> Thus, a modest amount of heating or incomplete thermalization of the spin population of the acceptor level causes this component to dominate, given the relatively small strain splitting. We have performed line-shape fits to the  $e-A^0$  peaks using Eq. (2), incorporating strain splitting of the acceptor level and the difference in oscillator strengths, as well as the effects of thermalization, assuming for simplicity equal electron and hole temperatures. The results are acceptable only if the heavy-hole component is allowed to dominate. Moreover, we have recently observed a well-resolved strain splitting of the shallow acceptor level in similarly strained P-doped ZnSe, in which the heavy-hole component is found to become dominant above about 10 K.<sup>39</sup> For these reasons, we conclude that our observed peaks all involve the heavy-hole acceptor level in the Li-doped material, which implies that the strain splitting of the acceptor level must be added to 111.9 meV to obtain the true light-hole acceptor binding energy.

The splitting of an acceptor level subject to a  $\langle 100 \rangle$  strain ( $\Delta E_A$ ) can be calculated using perturbation theory within the effective-mass model of the acceptor states as  $\Delta E_A = (b'/b)\Delta E_v$ , where  $\Delta E_v$  is the splitting of the valence band, and  $b'$  and  $b$  are the shear deformation potentials of the acceptor-bound and free holes.<sup>40</sup> Using the Luttinger parameters given in Ref. 41, we obtain  $\mu = (6\gamma_3 + 4\gamma_2)/5\gamma_1 = 0.49$  and  $\delta = (\gamma_3 - \gamma_2)/\gamma_1 = 0.18$ . Thus,  $b'/b = 1 - 4\mu^2/5 - 12\mu\delta/25 = 0.77$ .<sup>40</sup> From the splitting of the heavy- and light-hole free excitons we have  $\Delta E_v = 2.8$  meV, so that  $\Delta E_A = 2.2$  meV. When this value is added to 111.9 meV, we find the true value of  $E'_A$  (the acceptor binding energy in strained material) to be 114.1 meV. To find the binding energy in unstrained material,  $E_A$ , we use the relation<sup>40</sup>

$$E_{A'} = E_A + \frac{\Delta E_v}{2} \left[ \frac{b'}{b} - 1 \right] + \frac{(\Delta E_v)^2}{4E_A} \left\{ 1 - \left[ \frac{b'}{b} \right]^2 \right\}. \quad (4)$$

The third term on the right-hand side of Eq. (4) is relatively small compared to the second term and is neglected. Using  $E'_A = 114.1$  meV, we find  $E_A = 114.4 \pm 0.4$  meV, based on data from four samples. The strain

correction is thus essentially negligible. Our value is in good agreement with the value of 114 meV previously reported in the literature,<sup>2</sup> based on the curve fitting of discrete ( $D^0-A^0$ ) pair lines at large pair separations in unstrained material, and with the value of 113.4 meV found in Ref. 42 for strained material based on electronic Raman-scattering measurements. Our direct measurement technique, however, does not depend on any assumptions about the dielectric constant or the donor binding energy.

Figure 3 shows that the FWHM of the  $e-A^0$  peak in our material (plotted as circles) increases linearly with temperature. A fit to our data (the solid line in Fig. 3) gives an intercept of 2.4 meV and a slope of 0.21 meV/K. From Eq. (2), we find that the FWHM of the peak is theoretically about  $1.8k_B T$ , assuming a single dominant strain-split component. The slope of the fitting line agrees approximately with the theoretical value of  $1.8k_B = 0.16$  meV/K. The slightly larger value we find may be due in part to inhomogeneous strain broadening that increases with temperature, due to thermalization. The agreement with theory once again verifies our assignment of the  $e-A^0$  peak. However, the intercept of the fitting line does not coincide with the theoretical value of zero. This discrepancy may be partly due to the strain splitting of the acceptor level as well as inhomogeneous strain broadening in the heteroepitaxial material, resulting from the strain fields associated with misfit dislocations.<sup>34,43,44</sup> An estimate of the inhomogeneous strain broadening is available from the Li-acceptor-bound-exciton linewidths, which are approximately 1 meV in this sample. Thus, we conclude that part of the broadening is due to this mechanism, and some may also result from the  $\sim 2$  meV strain splitting. Other possible broadening mechanisms include tailing of the conduction band due to the excited states of donors that have merged with it, and errors involving our assumption that the electron temperature equals the lattice temperature.

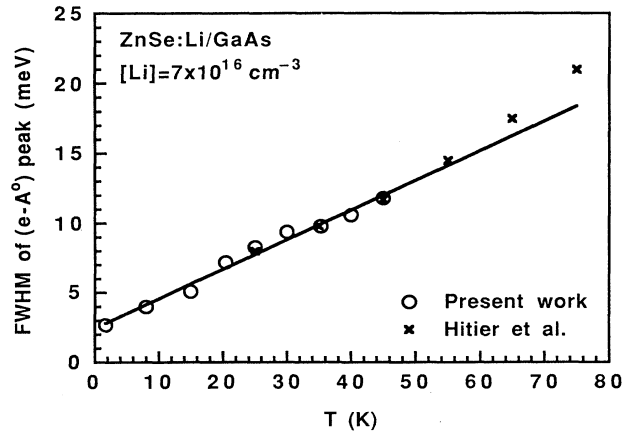


FIG. 3. The FWHM of the  $e-A^0$  peak as a function of sample temperature for the sample of Fig. 1 (circles), together with a linear fit to the data (solid line) as described in the text. The crosses represent the corresponding data of Ref. 30 for bulk material.

We have also plotted as the crosses in Fig. 3 the FWHM of the  $e-A^0$  peak measured as a function of temperature ( $\geq 25$  K only) in bulk material by Hitier, Canny, and Rommeluere<sup>30</sup> for an acceptor believed to be Li. Their data are in excellent agreement with ours from 25–45 K (the region of overlap). A linear fit to their data (not shown) over the range 25–77 K yields a slope of 0.26 meV/K and an intercept of 0.8 meV. The intercept is smaller in bulk material, perhaps corresponding to a reduction in strain broadening, although the slope is somewhat larger than the theoretically expected value. Above 45 K, therefore, an additional temperature-dependent broadening mechanism may be present.

One possible broadening mechanism in this strongly polar II-VI material is that due to coupling of the localized acceptor-bound hole with low-energy acoustic phonons. However, the narrow linewidths ( $\sim 2$  meV) of the discrete  $D^0-A^0$  pair lines discussed below, which should have comparable or stronger phonon coupling, lead us to conclude that this mechanism is not very significant. Our results (specifically the fits of Figs. 2 and 3) demonstrate clearly that the concerns expressed by Dean and Merz<sup>1</sup> regarding the influence of phonon coupling on the determination of shallow acceptor binding energies from  $e-A^0$  peak positions in ZnSe are unfounded, at least at reasonably low temperatures, and that this technique is in fact the most direct and accurate one available for determining acceptor binding energies.

### B. Anomalous temperature dependence of the $e-A^0$ and $D^0-A^0$ peaks

An anomalous initial decrease in the intensity of the  $e-A^0$  peak with respect to that of the  $D^0-A^0$  peak is observed for temperatures below 15 K, as shown in Fig. 1. As the temperature increases, the intensities of both the  $e-A^0$  and the  $D^0-A^0$  peaks quench. However, the  $e-A^0$  peak quenches faster than the  $D^0-A^0$  peak. This decrease of the  $e-A^0$  peak relative to the  $D^0-A^0$  peak has not previously been reported for III-V or II-VI materials, to our knowledge.

In order to understand this behavior, we have developed a simple model based on the following assumptions: (1) The donors and the conduction band are in quasiequilibrium with one another, with a common electron temperature  $T_e$  and a quasi-Fermi level  $E_{Fn}$ . The electron temperature is assumed to equal the lattice temperature for simplicity. (2) The radiative lifetime for electrons undergoing  $e-A^0$  transitions is a temperature-independent constant  $\tau_{eA}$ ; the assumed constant concentration of neutral acceptors ( $N_A^0$ ) is incorporated into this lifetime. The assumption of constant  $\tau_{eA}$  should be valid in the range of interest, according to the theory of Eagles,<sup>31</sup> given the assumption of constant  $N_A^0$ , which should be reasonable in  $p$ -type material, especially for low excitation. (3) The average lifetime of electrons on donors due to donor-acceptor pair recombination is a constant,  $\langle \tau_{DA} \rangle$ . This assumption is valid for constant  $N_A^0$  as long as the shape and position of the  $D^0-A^0$  pair peak remain constant with respect to the band edge, since photon energy is related to pair separation, which in turn

determines the oscillator strength. We indicate below where this assumption holds and where it fails. (4) Electrons in the conduction band or on donors have nonradiative lifetimes, which for convenience we parametrize in the forms

$$\begin{aligned}\tau_{nr}^1 &= C_1 \tau_{eA} \exp(E_a/k_B T_e), \\ \tau_{nr}^2 &= C_2 \langle \tau_{DA} \rangle \exp(E_a/k_B T_e),\end{aligned}$$

respectively, where  $C_1$  and  $C_2$  are constants and  $E_a$  is a constant activation energy. For simplicity we use the same value of  $E_a$  for both electron populations, although this may not be true. These “nonradiative” rates also include any competing radiative recombination pathways that do not contribute to the  $D^0-A^0$  or  $e-A^0$  emission intensities, such as capture of free electrons to form excitons and their subsequent recombination.

With the above assumptions, the constant optical volume generation rate  $G$  must balance the total radiative and nonradiative recombination rates at any temperature, so that

$$G = \frac{n}{\tau_{nr}^1} + \frac{N_D^0}{\tau_{nr}^2} + \frac{n}{\tau_{eA}} + \frac{N_D^0}{\langle \tau_{DA} \rangle} \quad (5)$$

The observed integrated intensities of the  $e-A^0$  and  $D^0-A^0$  peaks are then given by  $I_{e-A^0} = Cn/\tau_{eA}$  and  $I_{D^0-A^0} = CN_D^0/\langle \tau_{DA} \rangle$ , respectively, where  $C$  is a constant,  $n$  is the free-electron concentration, and  $N_D^0$  is the neutral donor concentration. For nondegenerate semiconductor statistics we have  $n = N_c \exp(E_{Fn}/k_B T)$  and  $N_D^0 = N_D \{1 + (\frac{1}{2}) \exp[(-|E_D| - E_{Fn})/k_B T]\}^{-1}$ , where  $N_c$  is the effective density of states in the conduction band,  $E_D$  is the donor binding energy, and a degeneracy of two is assumed for the shallow donors. The excited states of the donors are ignored. Substituting the expressions for  $n$  and  $N_D^0$  into Eq. (5), we obtain a quadratic equation that is easily solved for  $E_{Fn}$  as a function of temperature, which in turn yields the integrated intensities of the  $e-A^0$  and  $D^0-A^0$  peaks according to the relations given above.

In Fig. 4, we have plotted the measured integrated  $e-A^0$  and  $D^0-A^0$  peak intensities as the points denoted  $o$  and  $x$ , respectively, for a sample grown at 260°C with  $[Li] = 3.8 \times 10^{17} \text{ cm}^{-3}$  and  $N_A - N_D = 8.0 \times 10^{15} \text{ cm}^{-3}$ . The intensities were determined using least-squares fits of theoretical line shapes to the data. We performed a fit to the data in Fig. 4 using Eq. (5), in which a total of seven unknown parameters were varied. The best fit we obtained is shown as the lines in Fig. 4, where we have plotted normalized quantities proportional to each term of Eq. (5) as a function of temperature. The solid lines are the nonradiative and radiative recombination rates of electrons on donors, while the dashed lines are the same two quantities for free electrons. The dotted line is the generation rate, which equals the sum of the other four quantities as required. Note that “nonradiative” (i.e., competing) recombination is dominant for both free and bound electrons, due to the importance of excitonic recombination and the true nonradiative recombination in this heteroepitaxial sample grown at low temperature.

The fact that samples grown at higher substrate temperatures have seven times larger integrated spectral intensities under identical conditions is consistent with the dominance of nonradiative recombination in the present case.

The “nonradiative” lifetimes for both free and donor-bound electrons become shorter with increasing temperature, but only the nonradiative recombination rate involving the donor-bound electrons actually increases with temperature, because of the reduction in  $n$  (which is proportional to the lowest, dashed curve) with increasing  $T$ .

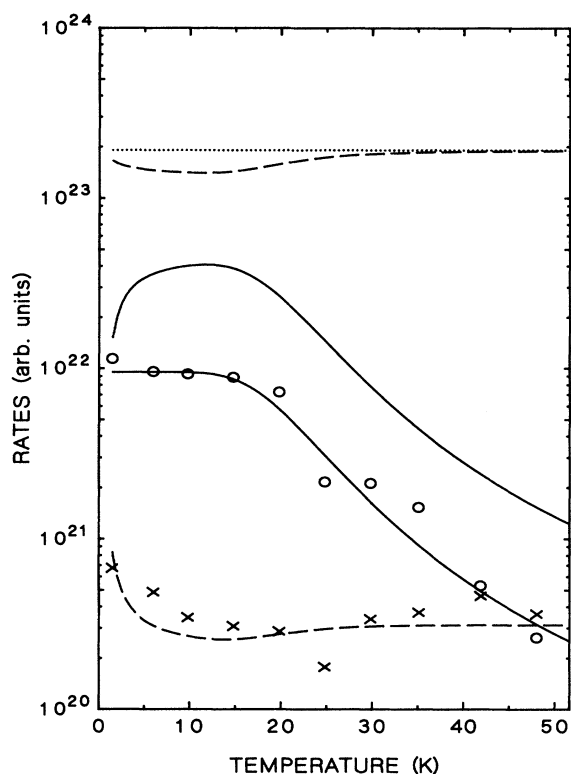


FIG. 4. Radiative and “nonradiative” recombination rates for  $D^0-A^0$  (solid lines) and  $e-A^0$  (dashed lines) recombination determined by fitting Eq. (5) to the experimental integrated peak intensities for the sample described in the text, which are shown on the figure as “o”  $D^0-A^0$  and “x”  $e-A^0$ , respectively. The uppermost dotted line is the constant generation rate. All rates have been multiplied by  $\tau_{eA}$ . The upper dashed and solid curves are for the “nonradiative” processes, while the lower dashed and solid curves are the radiative ones. The parameters obtained from the fit are the following:  $G\tau_{eA} = 1.9 \times 10^{17} \text{ cm}^{-3}$ ,  $C_1 = 0.0016$ ,  $C_2 = 0.198$ ,  $E_a = 0.15 \text{ meV}$ ,  $C = 6.5 \times 10^{-14} \text{ cm}^3$ ,  $N_D\tau_{eA}/\langle\tau_{DA}\rangle = 9.5 \times 10^{15} \text{ cm}^{-3}$ , and  $|E_D| = 7.5 \text{ meV}$ . The value of  $|E_D|$  is substantially less than the accepted hydrogenic value of about 28 meV, which may be due in part to conduction-band tailing but is probably mainly a consequence of changes in  $\langle\tau_{DA}\rangle$  above 25 K which are not included in the model. The reduced intensities of the neutral donor-related rates above 15 K and the corresponding rises in the free-electron-related rates are due to thermal ionization of the donors into the conduction band. The initial drop in  $e-A^0$  peak intensity is a result of the temperature-dependent nonradiative rates, as discussed in the text.

The main point to note is that the reduction in nonradiative lifetimes with increasing  $T$  has given rise theoretically to a reduction in  $e-A^0$  peak intensity with increasing  $T$  in the low-temperature range, followed by an increase at higher temperatures. Both of these predictions are qualitatively in accord with the experimental data. The decrease in intensity at the highest temperatures (above 42 K) is due to thermal ionization of the shallow acceptors, which is not included in our model. By varying parameters in the model, we find that the experimentally observed decreasing  $e-A^0$  peak intensity at low temperature can only be obtained using nonradiative lifetimes that decrease with  $T$  in this range. The assumption of constant  $D^0-A^0$  peak position and shape is valid only up to about 25 K in this sample, which probably accounts for the unrealistically low donor ionization energy required to fit the data in this range (see the caption of Fig. 4).

While the detailed fits obtained above should not be taken too seriously, due to the number of unknown parameters and the somewhat arbitrary assumptions we have made, the qualitative result that temperature-dependent nonradiative recombination can account for the initial anomalous decrease in  $e-A^0$  peak intensity with increasing temperature is clearly established.

### C. Identification of the Li acceptor level

There is still some controversy in the literature concerning the binding energy of the Li acceptor level, even in recent work,<sup>11</sup> and its level seems to have been frequently confused with that of Na.<sup>3,4,9</sup> Several factors appear to have contributed to this controversy. First, the positions of nonresonantly excited  $D^0-A^0$  pair peaks have often been used for identification purposes, particularly since  $e-A^0$  peaks are not normally observed at low temperature. The positions of these  $D^0-A^0$  peaks shift as a function of excitation level, doping, and donor species, which in turn vary from study to study. Second, Na frequently does not incorporate well in ZnSe, even in intentionally Na-doped material, probably due to its large covalent radius; this factor must be taken into account. Finally, the binding energy of Li has frequently been determined using techniques that are inherently inaccurate, such as the use of acceptor-bound exciton peak positions in conjunction with “Haynes’s rule,” and analysis of  $D^0-A^0$  peak positions without an accurate knowledge of the Coulomb interaction.

Haynes’s rule (i.e., that the localization energy of a bound exciton on an impurity varies linearly with impurity binding energy, with a slope of about 0.1) is valid for Si and some other indirect materials,<sup>45,46</sup> but is known to be completely invalid for common shallow acceptors in direct gap III-V and II-VI materials, where the variation in exciton localization energy with acceptor binding energy is typically weak and not even linear.<sup>46</sup> The breakdown of the “normal” linear relationship is generally attributed to the importance of interparticle correlations in the binding of excitons to neutral acceptors.<sup>46</sup> An early study by Halsted and Aven<sup>47</sup> concluded that Haynes’s rule applied to acceptor levels in many II-VI materials,

but the correlation between bound excitons and corresponding acceptor peaks was not well established at the time of that study, let alone the chemical identification of those acceptors. Moreover, it was based on data for relatively deep levels, and more recent work has shown that the relationship between acceptor binding energy and exciton localization energy for shallow acceptors is actually retrograde,<sup>48</sup> and nonlinear when data on shallow P-related acceptors are included.<sup>39,49</sup> While it happens to be true that the exciton localization energy is about 10% of the acceptor binding energy for several shallow acceptors in ZnSe taken as a group, there is no *linear* relationship between these two quantities for *individual* shallow acceptor levels. Therefore, Haynes's rule is not a reliable and accurate way to determine differences between binding energies of acceptor levels such as Li or Na, which are separated by only about 12 meV. It should never be used to predict or determine acceptor binding energies, if any significant degree of accuracy is desired.

One of the transitions believed to involve substitutional  $\text{Li}_{\text{Zn}}$  acceptor levels is the so-called *R* band, first reported by Dean and Merz in bulk ZnSe.<sup>1</sup> The position of this peak is reported to vary over a wide range ( $2.707 \pm 0.003$  eV), depending on the study in question, and it frequently appears in conjunction with the *Q* band involving ( $\text{Al}_{\text{Zn}} - \text{Li}_{\text{Zn}}$ ) transitions. It does not exhibit discrete pair lines, or a corresponding  $e-A^0$  peak at high temperature.<sup>1</sup> It is significantly broader than the *Q* band, and exhibits comparable or even slightly stronger LO-phonon coupling,<sup>1</sup> both of which would be surprising if it simply involved a shallower acceptor level. Tews, Venghaus, and Dean concluded from selective pair luminescence (SPL) measurements of the *R* band that it involves substitutional  $\text{Li}_{\text{Zn}}$  acceptors and a hydrogenic shallow donor.<sup>50</sup> Bhargava *et al.*<sup>5</sup> studied Li- and Na-doped bulk material and

concluded that the *R* band is a transition between preferentially paired interstitial Li donors and substitutional  $\text{Li}_{\text{Zn}}$  acceptors. However, we have not observed this *R* band in any Li-doped samples grown by MBE under various growth conditions, even in the highly compensated sample with a Li concentration of  $4.9 \times 10^{19} \text{ cm}^{-3}$  and a hole concentration less than  $10^{15} \text{ cm}^{-3}$ . This result raises questions about the model of Ref. 5 for the *R* band, which seems to appear only in bulk material containing many Na and other impurities as well as naive defects, and has not been observed so far in either doped or undoped material grown by MBE.

The binding energies of Li acceptors obtained by various researchers are shown in Table I. Dean and Merz<sup>1</sup> and Merz, Nassau, and Shiever<sup>2</sup> studied bulk material and observed two distant  $D^0-A^0$  peaks denoted *R* and *Q*, and a series of discrete lines which appeared under high excitation. By fitting the positions of these discrete  $D^0-A^0$  lines, they deduced a value of  $E_D + E_A = 140$  meV using a relative dielectric constant of 8.66; they obtained  $E_A^{\text{Li}} = 114$  meV by subtracting the binding energy of the donor,<sup>2</sup> in good agreement with the present work. Their observation of an isotope shift in the discrete  $D^0-A^0$  pair lines provided indisputable evidence for the involvement of Li in the spectrum.<sup>2</sup> Chatterjee, Rosa, and Streetman<sup>3</sup> estimated an acceptor binding energy of 102 meV from a band-to-acceptor peak observed at 77 K for an acceptor level believed to be Na. From the peak positions in their PL spectra, we feel (in agreement with Bhargava *et al.*<sup>5</sup>) that the peaks they assigned as *R* and *Q* are probably the *Q* and *P* peaks of Merz, Nassau, and Shiever, and the band-to-acceptor peak probably corresponds to the acceptor level of the *Q* peak. Therefore, the binding energy of the acceptor should be that of Li, even though it does not seem to have been determined accurately from the

TABLE I. Binding energy of Li acceptor in ZnSe.

	Binding energy of Li (meV)	Analysis technique
Dean and Merz (Ref. 1)	114	Discrete $D^0-A^0$ pair (DAP) lines $E_D + E_A = 140$ meV
Merz, Nassau, and Shiever (Ref. 2)	114	Discrete DAP lines
Chatterjee, Rosa, and Streetman (Ref. 3)	102	Band-to-acceptor peak Assigned to Na
Swaminathan and Greene (Ref. 4)	113	Discrete DAP lines Assigned to Na $E_D + E_A = 139$ meV
Cheng <i>et al.</i> (Ref. 12)	115	Haynes's rule
Ohishi (Ref. 9)	113.4–114.2	Time-resolved SPL Assigned to Na
Isshiki <i>et al.</i> (Ref. 11)	105	Estimate from donor-to-acceptor peak
Olego <i>et al.</i> (Ref. 42)	113.4	Electronic Raman scattering
Hingerl <i>et al.</i> (Ref. 20)	113	Haynes's rule
Fan and Woods (Ref. 51)	117	Band-to-acceptor peak
Yoshikawa <i>et al.</i> (Ref. 52)	101/118	Haynes's rule/estimate from $D^0-A^0$ peak position
Present work	114.5	Intercept of fitting line for $e-A^0$ peak position



peak position. Swaminathan and Greene<sup>4</sup> studied the PL properties of melt-grown ZnSe. From observations of discrete  $D^0-A^0$  lines they obtained  $E_D + E_A = 139$  meV and suggested that the donor was Al and the acceptor was a Na-related complex. However, the value of  $E_D + E_A$  is very close to the value of that involving the Li acceptor reported by Merz, Nassau, and Shiever, and we feel the acceptor should be Li. Fan and Woods determined a binding energy of 117 meV from an  $e-A^0$  peak position at 25 K;<sup>51</sup> however, reanalyzing their data with the value of  $E_g$  used here for unstrained material [see Eq. (1)] yields 113.9 meV, in good agreement with other determinations.

Cheng *et al.*,<sup>12</sup> Hingerl *et al.*,<sup>20</sup> and Yoshikawa *et al.*<sup>52</sup> calculated the binding energy of Li in Li-doped material by using Haynes's rule. As we discussed above, Haynes's rule cannot give reliable and accurate values to distinguish different shallow acceptor levels. Yoshikawa *et al.* also made an estimate based on the  $D^0-A^0$  peak position,<sup>52</sup> but did not have an accurate way of determining the Coulomb term. Ohishi<sup>9</sup> obtained an acceptor binding energy of 113.4–114.2 meV from time-resolved selective pair luminescence. Since only Na was detected and no Li was found by ion microanalysis (IMA) of the sample, they concluded that Na is responsible for the acceptor level. This value is exactly the binding energy of Li reported in the literature and agrees with the present work. Therefore, the acceptor in that sample appears to be Li. Although Na was detected, it may not have been located on Zn sites; moreover, the sensitivity of the IMA may have been insufficient to detect the presence of Li.

Isshiki *et al.*<sup>11</sup> studied the PL of Li-doped ZnSe single crystals and observed the  $Q$  peak with a no-phonon position of 2.6923 eV. By arguing that the Coulomb term was lower than the experimental error at a low excitation level at which the  $D^0-A^0$  peak position appeared to reach a low-energy limit, they obtained a value of  $E_D + E_A = 133 \pm 1$  meV. Considering the binding energy of the donor, a binding energy for Li of 105 meV was obtained, which is smaller than the value obtained in most other work. Clearly, the assumption of a negligible Coulomb term is not valid, since their value conflicts with the one determined here in a more direct way. The nature of the Poisson distribution of interimpurity separations insures that there will always be significant Coulomb interaction at the maximum of the  $D^0-A^0$  peak. Olego *et al.*<sup>42</sup> observed a peak assigned to acceptor-to-valence-band transitions in electronic Raman-scattering measurements on Li-doped heteroepitaxial ZnSe grown by MBE and obtained a binding energy for Li of 113.4 meV. This value is in reasonable agreement with the values reported in the literature and in the present work.

#### D. Magnetoluminescence

Magnetoluminescence measurements of band-to-acceptor peaks have been reported previously in bulk GaAs,<sup>37,53–55</sup> GaSb,<sup>56,57</sup> ZnTe,<sup>24</sup> and CdTe,<sup>58</sup> as well as in  $\text{Al}_x\text{Ga}_{1-x}\text{As}/\text{GaAs}$  superlattices.<sup>38</sup> A preliminary study of this type was also reported by Skromme *et al.* for an  $e-A^0$  peak involving a residual shallow (probably

As-related) acceptor level in  $n$ -type heteroepitaxial ZnSe on GaAs, measured at an elevated temperature (38 K).<sup>35</sup> These results showed that the  $e-A^0$  peak in all of these materials becomes narrower and shifts linearly to higher energy with increasing magnetic field, reflecting the field dependence of the lowest Landau level and its associated density of states.

Luminescence spectra as a function of magnetic field from 0 to 12 T in  $\sigma^+$  polarization are shown in Fig. 5 for the sample of Fig. 1, together with a  $\sigma^-$  polarized spectrum at 12 T. The positions of the  $D^0-A^0$  and  $e-A^0$  peaks in corresponding unpolarized data in Faraday ( $\sigma^+/\sigma^-$ ) configuration are plotted in Fig. 6. No splitting between the  $\sigma^+$  and  $\sigma^-$  components of the Li  $e-A^0$  peak is detectable in our low-temperature data up to 12 T. We note first that the  $D^0-A^0$  pair peak shifts slowly and nonlinearly to higher energy with field, as previously observed in several other cases.<sup>38,53,54,58</sup> This shift is ascribed to the diamagnetism of the shallow donor level, with an additional contribution from a shift toward recombination at closer pairs, due to the shrinkage of the donor wave function and the resulting increase in radiative lifetime for the more distant pairs.

In the low-magnetic-field region ( $\leq 4$  T), we observe a nonlinear diamagnetic shift to higher energy for the  $e-A^0$  peak, which has been reported before in other systems,<sup>38,55</sup> and is due to the field-induced changes in the density of states in the conduction band. For higher

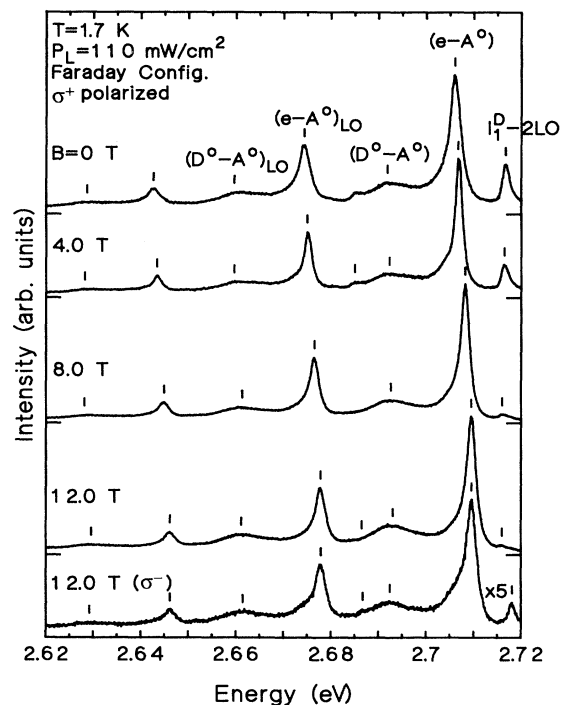


FIG. 5. Low-temperature magnetoluminescence spectra under blue excitation at 2.816 eV of the  $e-A^0$  peak for the sample of Fig. 1. The spectra for  $B=0-8$  T are  $\sigma^+$  polarized, and both  $\sigma^+$ - and  $\sigma^-$ -polarized spectra are shown for 12 T. The intensity of the  $\sigma^-$ -polarized spectrum at 12 T is five times weaker than that of the  $\sigma^+$ -polarized spectrum at 12 T. Instrumental resolution is 0.2 meV or better.



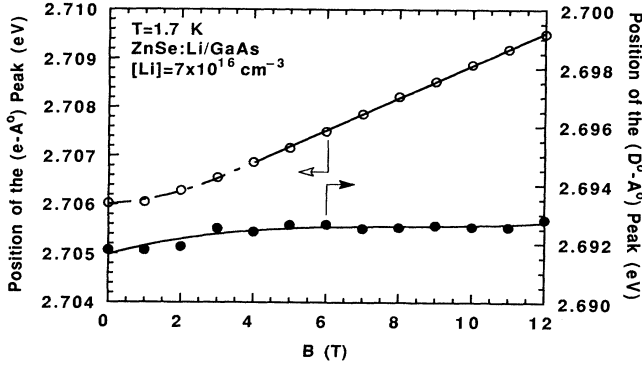


FIG. 6. Position of the  $e-A^0$  and  $D^0-A^0$  peaks as a function of magnetic field for the sample of Fig. 1 (open and filled circles, respectively). The solid line plotted through the  $e-A^0$  points is a linear fit to the data in the high-magnetic-field region ( $B \geq 4$  T), while the dashed line for  $B \leq 4$  T is only a guide to the eye. The line through the  $D^0-A^0$  points is merely a guide to the eye.

magnetic field ( $\geq 4$  T), we observe a linear shift of the  $e-A^0$  peak with field, which corresponds to the  $\hbar\omega_c/2$  shift (neglecting nonparabolicity) of the lowest ( $n=0$ ) Landau level in the conduction band ( $\omega_c = eB/m_e^*$  is the cyclotron frequency,  $e$  is the electronic charge, and  $m_e^*$  is the polaron mass). We neglect higher-order polaron effects, beyond using the renormalized polaron mass, since they are found to be unimportant as previously determined in ZnTe.<sup>24</sup> In principle, this linear shift should include spin splittings of both electron and hole and the “diamagnetic splitting” of the hole, but as discussed below we believe that these splittings are insignificant in our data. The diamagnetic shift of the acceptor level is expected to be negligible in ZnSe, since it is already nearly negligible ( $< 0.1$  meV) even for the much shallower  $C$  acceptors in GaAs.<sup>37</sup> Unlike previous measurements on GaAs,<sup>37,55</sup> ZnTe,<sup>24</sup> and CdTe,<sup>58</sup> we find it possible to observe only the  $n=0$  Landau level under most conditions, presumably due to collision-induced broadening of the Landau levels and inhomogeneous strain broadening of the  $e-A^0$  peaks. Under carefully optimized conditions ( $B=12$  T and  $T=52$  K) we did manage to observe a shoulder at the expected position of the  $n=1$  level, but could not determine its position with high accuracy. Thus, we use only the  $n=0$  data in determining the effective mass below.

Using a least-squares fit to the points in the high-magnetic-field region ( $B \geq 4$  T), we obtain an effective polaron mass for the electrons of  $m_e^* = 0.17$ , which is in excellent agreement with Ref. 59. In principle, we should include the spin splittings of the electron and hole in the analysis, but we have not been able to achieve a satisfactory analysis of them. The peak positions in  $\sigma^+$ ,  $\sigma^-$ , and  $\pi$  polarizations (all with  $\mathbf{B} \parallel \langle 100 \rangle$ ) are all coincident within 0.1 meV at a given field in the range 0–12 T in low-temperature measurements, although we do find a

$\sim 0.8$  meV splitting between the  $\sigma^+$  and  $\sigma^-$  positions at higher temperatures ( $\sim 50$  K), with the  $\pi$  position occurring about halfway between them. From 0–4 T we observe significant narrowing of the  $e-A^0$  peaks from FWHM=3.2 to 2.0 meV, consistent with the change in the conduction band density of states in the field, but for 4–12 T the  $e-A^0$  peaks broaden monotonically with field in all three polarizations ( $\sigma^+$ ,  $\sigma^-$ , and  $\pi$ ). The broadening might suggest unresolved spin splittings, but these should be observable as splittings in the peak positions. We have not been able to achieve a fully satisfactory explanation of these results for any combination of electron and hole  $g$  factors, including the inevitable strain splitting of the acceptor level. The best analysis assumes very small ( $\ll 1$ )  $g$  factors for both electron and hole, which is, however, inconsistent with magnetorefectance measurements of the  $g$  factor of electrons in free excitons,<sup>41</sup> which should be fairly close to that of free electrons. Even assuming small  $g$  factors the field-induced broadening and intensify difference between  $\sigma^+$  and  $\sigma^-$  components (see Fig. 5) remain unexplained. We hope to achieve a better resolution with measurements on P-doped material, which are in progress.

Low-temperature PL spectra under low excitation for the most heavily Li-doped sample are shown in Fig. 7 for both zero and high magnetic field. In the  $B=0$  spectrum, the  $e-A^0$  peak appears to have some unresolved broadening on the low-energy side, since it does not ex-

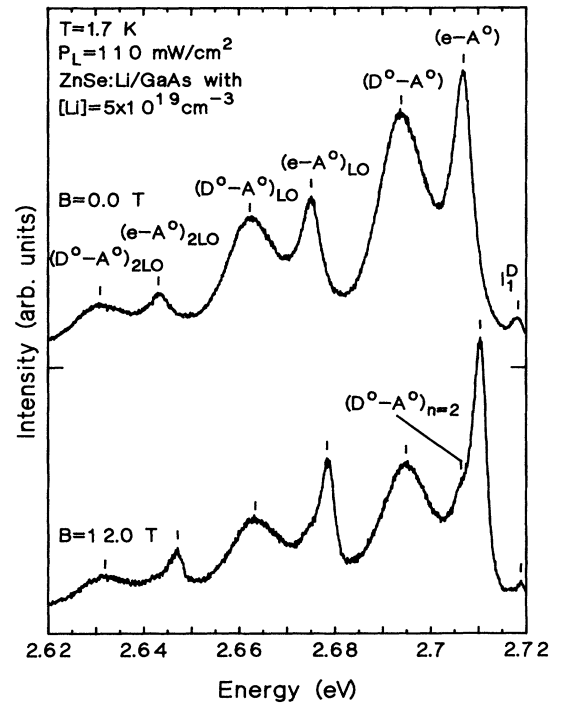


FIG. 7. A portion of the low-temperature PL spectra under UV excitation in magnetic fields of 0 and 12 T for the most heavily doped ZnSe/GaAs layer, which has a total Li concentration of  $5 \times 10^{19} \text{ cm}^{-3}$  and  $|N_A - N_D|$  less than  $10^{15} \text{ cm}^{-3}$ . Instrumental resolution is 0.27 meV or better.

hibit the sharp cutoff expected according to Eq. (2). Similar broadening was observed in the case of ZnTe by Dean, Venghaus, and Simmonds, who ascribed it to collisional (lifetime) broadening of the free-electron states.<sup>24</sup> At high magnetic field in Fig. 7, however, this “broadening” is resolved into a distinct shoulder. Judging by the position (about  $\frac{3}{4}$  of the way from the  $D^0-A^0$  to the  $e-A^0$  peak) and intensity of this peak, and comparing it to previous observations and calculations at  $B=0$  in GaAs and InP,<sup>25</sup> we assign it to a transition involving normal shallow donors in their first ( $2p^-$ ) excited state and Li acceptors in their ground state, denoted  $D_{n=2}^0-A^0$  recombination. Only the lowest ( $2p^-$ ) component of the  $n=2$  donor level is observed, due to thermalization and broadening from the Coulomb interaction. This feature is clearly detected only at high field, due to the reduction in the linewidth of the  $e-A^0$  peak and the shift of the  $e-A^0$  peak away from the ground-state  $D^0-A^0$  peak. An assignment of this peak to a light-hole acceptor level is ruled out by the magnitude of the strain splitting that would be implied. At  $B=0$ , the donor excited states (together with any band tailing that may be present) merely contribute to the unresolved low-energy broadening of the  $e-A^0$  peak. Part of the difficulty in resolving the  $D_{n=2}^0-A^0$  peak in that case is no doubt related to the inhomogeneous strain broadening present in these samples.

### E. PL properties as a function of growth conditions

Low-temperature PL spectra under low excitation of four comparably Li-doped samples grown at different substrate temperatures are shown in Fig. 8. As the growth temperature increases, the relative intensity of the

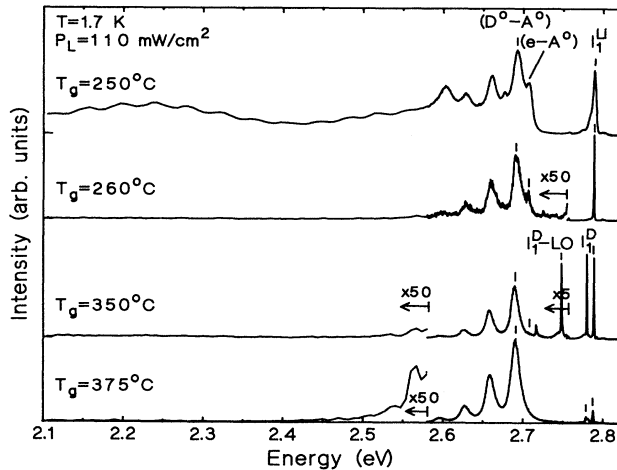


FIG. 8. Low-temperature PL spectra under low-level UV excitation for ZnSe/GaAs samples grown at different temperatures, with total Li concentrations of  $1.0 \times 10^{18}$ ,  $3.8 \times 10^{17}$ ,  $1.2 \times 10^{17}$ , and  $1.0 \times 10^{18} \text{ cm}^{-3}$ , listed in order of increasing growth temperature. The  $|N_A - N_D|$  values for these samples are less than  $10^{15}$  (i.e., fully depleted),  $8 \times 10^{15}$ ,  $5 \times 10^{16}$ , and  $6 \times 10^{15} \text{ cm}^{-3}$ , respectively. The spectra are corrected for the system response.

excitonic emission first increases, then decreases. The Li acceptor-bound exciton peak (labeled  $I_1^{Li}$ ) is significantly broadened at the lowest temperature, perhaps due to degraded crystal quality, and a bound exciton usually associated with Cu (Ref. 27) (labeled  $I_1^D$ ) appears in the samples grown at higher temperatures. The latter peak is often observed in ZnSe annealed at high temperature, and seems to require the presence of Zn vacancies for its formation.<sup>60-62</sup> As the temperature increases, the intensity of the  $e-A^0$  and  $D^0-A^0$  peaks decreases relative to that of the excitons, then increases at the highest substrate temperature. However, the total integrated intensity of the PL spectrum over the range 1.549–2.82 eV increases monotonically with growth temperature up to 375°C. The behavior of the total integrated intensity at both low and room temperatures will be discussed in detail elsewhere. Strong deep-level emission appears only at the lowest growth temperature. However, it is not entirely clear from the present data if the dramatic differences between the samples grown at 250 and 260°C are entirely due to the small change in substrate temperature, or to some other uncontrolled change in growth conditions. In this series of spectra,  $e-A^0$  peaks are observable only for the lower growth temperatures, while only  $D^0-A^0$  pair recombination is evident at the highest temperatures. The same result was found for all of the Li-doped samples we examined.

Figure 9 shows low-temperature PL spectra of four Li-doped samples with different Li-doping concentrations, grown at temperatures in the range 250–300°C and a Se/Zn flux ratio of 1:1, except for the sample of the top spectrum which had a flux ratio of 4:1. The excitonic emission becomes weaker as the Li concentration increases, and both the  $e-A^0$  and  $D^0-A^0$  peaks become stronger. The sample with  $[Li] = 1 \times 10^{18} \text{ cm}^{-3}$  shows

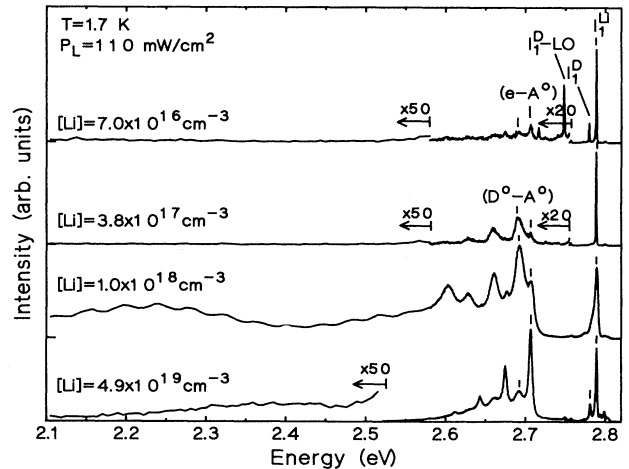


FIG. 9. Low-temperature PL spectra under low-level UV excitation for a series of ZnSe/GaAs samples as a function of total Li concentration. The corresponding  $|N_A - N_D|$  values for these samples are  $2 \times 10^{16}$ ,  $8 \times 10^{15}$ , less than  $10^{15}$  (i.e., fully depleted), and less than  $10^{15} \text{ cm}^{-3}$  in order of increasing Li concentration; the growth temperatures are 300, 260, 250, and 250°C, respectively. The spectra are corrected for the system response.

“anomalously” broad linewidths and strong deep-level emissions, although it is possible that these features could be uniquely related to this particular range of doping levels. The main point to note is that the  $e-A^0$  peak appears prominently, to varying degrees, in samples of various doping levels grown at 300 °C and below, and appears to be a frequently occurring feature in successfully  $p$ -type-doped ZnSe. It is, however, absent in samples grown at 350 °C and higher, which incidentally also have much lower nonradiative recombination rates. We believe that the  $e-A^0$  peak becomes observable at low temperature whenever the shallow donor concentration is low enough that the  $D^0-A^0$  pair recombination pathway is “saturated” by filling the donor levels even at low excitation levels, so that the additional photoexcited electrons are forced into the conduction band. This condition will not normally occur in  $n$ -type material, due to the higher donor concentration. In any case, it is clear that all future PL studies of  $p$ -type material must recognize the possibility of this peak occurring in the spectrum.

#### F. Discrete donor-acceptor pair spectra

A discrete  $D^0-A^0$  pair spectrum for the sample grown at 375 °C with a Li concentration of  $10^{18} \text{ cm}^{-3}$  is shown in Fig. 10. Tightly focused UV excitation is employed to emphasize the discrete structure. Discrete  $D^0-A^0$  pair lines have been observed several times in Li-doped bulk material,<sup>1,2,4</sup> and were first observed in heteroepitaxial ZnSe by Skromme *et al.* in a not intentionally doped MBE sample.<sup>24</sup> Subsequently, Shahzad *et al.* observed and attempted to analyze similar structure in  $N$ -implanted heteroepitaxial material.<sup>63</sup> The present results represent the first observation to our knowledge of discrete pair lines in Li-doped heteroepitaxial material. The spectrum is similar in form to the one shown in Fig.

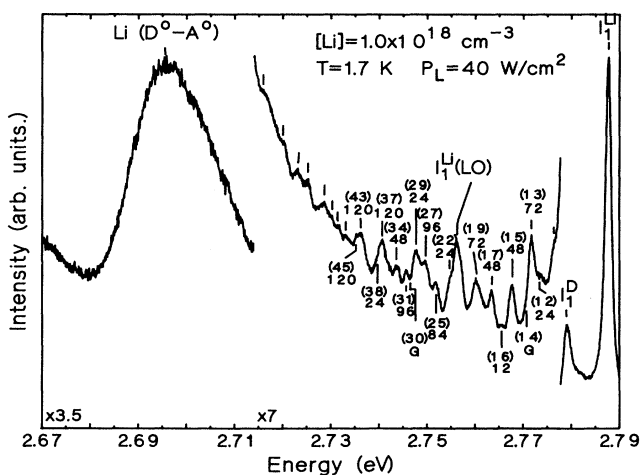


FIG. 10. Low-temperature PL spectrum under high-level UV excitation of the discrete donor-to-acceptor pair lines in ZnSe/GaAs sample with a total Li concentration of  $10^{18} \text{ cm}^{-3}$  and  $|N_A - N_D| = 6 \times 10^{15} \text{ cm}^{-3}$ . The instrumental resolution is 0.07 meV.

2 of Ref. 2 for type-I In-Li pairs in bulk material, except that the peaks are shifted down by about 3.3 meV in energy and are significantly broadened in the present case by the inhomogeneous strain. Based on this comparison, a tentative assignment of the shell numbers (in parentheses) is indicated in Fig. 10, together with the corresponding degeneracies. The degraded resolution does not allow a definite assignment. While the strain is expected to split the acceptor levels, only the lowest (light-hole) states should be observable at 1.7 K, the temperature used for the data of Fig. 10.

#### G. Li acceptor-bound excitons and local phonon modes

Variable-temperature PL spectra of the exciton region in a Li-doped sample with  $[\text{Li}] = 1.2 \times 10^{17} \text{ cm}^{-3}$  are shown in Fig. 11. Strain-split light- and heavy-hole free-exciton peaks ( $X_{lh}$  and  $X_{hh}$ ), a component of the Li acceptor-bound exciton at 2.7888 eV ( $I_1^{Li}$ ), a neutral or ionized donor-bound exciton peak at 2.7924 eV [ $I_3(?)$ ], a Cu acceptor-bound exciton ( $I_1^D$ ) at 2.7799 eV, and the LO-phonon replica of  $I_1^{Li}$  at 2.7570 eV are observed in the low-temperature spectrum. All of these peaks are shifted to lower energy with respect to their positions in bulk material,<sup>36</sup> due to the biaxial tensile thermal strain in this heteroepitaxial material.<sup>33-35</sup> With increasing temperature, an additional component of the Li

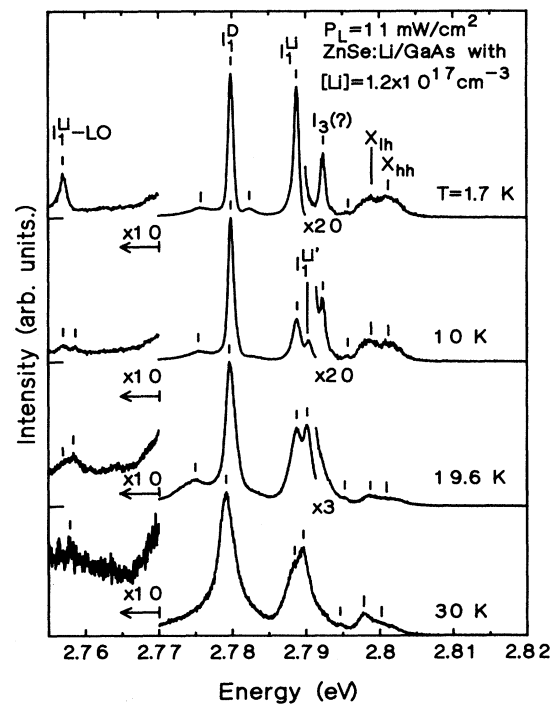


FIG. 11. PL spectra of the excitonic region as a function of temperature under low-level UV excitation for a 3.5  $\mu\text{m}$ -thick ZnSe/GaAs sample with a total Li concentration of  $1.2 \times 10^{17} \text{ cm}^{-3}$  and  $|N_A - N_D| = 5 \times 10^{16} \text{ cm}^{-3}$ . The instrumental resolution is 0.26 meV or better.

acceptor-bound exciton at 2.7904 eV ( $I_1^{\text{Li}'}$ ) becomes visible and even stronger than  $I_1^{\text{Li}}$  at the highest temperature. The LO-phonon replicas of the Li-acceptor-bound-exciton components below 2.76 eV also show the same behavior, which further proves that both components have a common origin, since their phonon-coupling strength is comparable. The substantial strength of the phonon coupling for these peaks is characteristic of tightly bound acceptor wave functions, and rules out the possibility that they are related to shallow donors. Our observation of a doublet is in agreement with previous studies,<sup>12,14-16,22</sup> as is the presence of thermalization.<sup>16</sup>

Calculations of the strain splittings and shifts for the Li acceptor-bound exciton are employed in the following to explain the existence of these strain-split components. Our analysis here parallels the one we gave recently for the acceptor-bound exciton in ZnTe;<sup>64</sup> the details of the model are given in that reference. The initial state of a neutral acceptor-bound exciton contains two holes and an electron. The two indistinguishable  $J=\frac{3}{2}$  holes are strongly coupled by an exchange interaction of strength  $\gamma$  to yield  $J=0$  and  $J=2$  states, which are the only ones allowed by the Pauli exclusion principle.<sup>65</sup> ( $\gamma$  is  $>0$  when the  $J=0$  state lies above  $J=2$ .) We neglect the small exchange interaction between the electron and the holes, due to the extended wave function of the electron in this complex, and we assume that the three distinct components of  $I_1^{\text{Li}}$  observed in unstrained bulk material<sup>66</sup> result from splitting of the  $J=2$  state by the cubic crystal field, along with the  $J=0$  state, which does not split. The magnitude of this splitting is denoted  $\beta$ , where  $\beta>0$  corresponds to the  $\Gamma_5$  state lying higher in energy than the  $\Gamma_3$  state. The final state is just a single  $J=\frac{3}{2}$  hole state in bulk material.

The three components of  $I_1^{\text{Li}}$  are reported to occur at about 2.7911, 2.7914, and 2.7916 eV in bulk material.<sup>66</sup> The peak positions are extracted from Fig. 5 in Ref. 66. Depending on the values of  $\gamma$  and  $\beta$ , there are seven possible orderings of the four energy levels, in which two of the energy levels are always degenerate. To achieve consistency with the bulk data, we find that four of these orderings are possible. These correspond to values of 0.34 or 0.27 meV for  $\gamma$  and 0.31 or  $-0.31$  meV for  $\beta$ , respectively, for the cases with  $\gamma>0$ , and values of  $-0.40$  or  $-0.37$  meV for  $\gamma$  and  $-0.15$  or 0.15 meV for  $\beta$ , respectively, for the cases with  $\gamma<0$ .

In a biaxial strain field, the initial state of the acceptor-bound exciton shifts and splits into four energy levels, which are parametrized by the values of  $\gamma$  and  $\beta$  determined above and by the hydrostatic deformation potential  $a$  and the shear deformation potential  $b'$ .<sup>67</sup> The latter value is reduced with respect to the value for free holes using perturbation theory for hydrogenically bound holes.<sup>40</sup> Identical values of  $b'$  are assumed in the initial and final states. The final neutral acceptor state simply splits into heavy- and light-hole levels in the biaxial strain field; we assume that, due to lifetime broadening in the upper level, only transitions involving the lower final level are observable. All of the possible transitions between upper and lower energy levels are allowed in our ( $\sigma$ ) configuration, according to group-theoretical arguments

similar to those given in Ref. 64.

Using the values of the Luttinger parameters from Ref. 41, the deformation potentials and elastic stiffness coefficients given in Ref. 43, together with the value of the biaxial strain determined from the free exciton splitting in Fig. 11 ( $\sim 0.5 \times 10^{-3}$ ), we calculate the expected peak positions in this strained material for all four possible models. Note that this calculation involves *no free-fitting parameters*. The best agreement (0.1 meV or better) with the two experimentally observed peak positions is found for  $\gamma=0.27$  meV and  $\beta=-0.31$  meV, where the two middle components which are separated theoretically by 0.31 meV are assumed to be unresolved experimentally. However, the other three models show discrepancies of at most 0.3 meV, which could easily be explained by experimental errors or small adjustments of deformation potentials. Thus, while we cannot positively distinguish among the various models based on our data, we can be confident that the observed components are due to strain splitting of the  $I_1^{\text{Li}}$  complex. Moreover, all of the quoted values for  $\gamma$  and  $\beta$  are plausible.

Physically, the observed peaks are roughly explained as transitions from initial states involving two light holes, and one heavy and one light hole to the final light-hole acceptor state, in order of increasing energy. The heavy-hole-light-hole state has unresolved splitting due to hole-hole or crystal-field coupling. The highest-energy peak predicted by the model involves an initial state with two heavy holes; it is experimentally unobservable due to thermalization, and because it is a "two-hole" transition which requires the nonrecombining hole to change its spin projection. While the peak labeled  $I_3(?)$  is almost exactly coincident with predicted position of this component, it is much too strong at low temperature relative to  $I_1^{\text{Li}'}$  to be consistent with an interpretation as a component of the  $I_1^{\text{Li}}$  peak. Further experiments are in progress to identify the exact nature of this peak. We have also calculated the expected magnetic-field splitting patterns in all four cases<sup>64</sup> and found them to be consistent with data we recorded in magnetic fields up to 12 T (not shown), within the experimental error and resolution. This result provides further confirmation of the possible models, although it does not indicate with certainty which one is correct.

Finally, we note that two sharp lines (not shown) were observed at 2.7421 and 2.7388 eV under resonant excitation at 2.7890 eV in the Li-doped sample with  $[\text{Li}]=3.8 \times 10^{17} \text{ cm}^{-3}$ . Peaks with spacings from  $I_1^{\text{Li}}$  within 0.2 meV of the above values were previously associated with local-phonon-mode replicas of that peak in Li-doped bulk material,<sup>68</sup> involving  $^6\text{Li}$  and  $^7\text{Li}$  isotopes. The absolute peak positions are of course different due to the strain shifts. The agreement in relative intensities (which reflect the expected natural abundance of the two isotopes) and in peak separations between our data and that in Ref. 68 clearly confirms the incorporation and activation of Li acceptors in this material.

#### H. Discussion of alternative models

In the following, we compare the above models of the strain splitting of the acceptor-bound exciton to those ad-

vocated by other authors. Our model is in distinct contrast to that advanced by Kudlek and co-workers<sup>69–72</sup> who claim, based on a measurement of relative oscillator strengths, that the doublet they observe in undoped ZnSe/GaAs is not due to strain splitting, but simply due to the exchange splitting between the  $J=0$  and  $J=2$  two-hole states. For this to be true, the shear deformation potential of the holes in the bound exciton complex would have to be almost totally quenched, for which they have offered no explanation. Such quenching was not observed in prior investigations of acceptor-bound excitons in GaAs,<sup>73</sup> InP,<sup>67</sup> GaSb,<sup>74</sup> and ZnTe,<sup>75</sup> for example. Moreover, the fact that the spacing of the doublet we observe in strained ZnSe:Li is several times larger than that in bulk material is incompatible with their model.<sup>76</sup> Also, the 1.2 meV  $J=0/J=2$  splitting cited by Kudlek *et al.*<sup>69</sup> for unstrained material applies to Na acceptors, which is unlikely to be the residual species they observed. Other acceptors may have smaller splittings in bulk material.<sup>66</sup> Thus, we conclude that the strain splittings of the holes in the bound-exciton complex must be considered in the analysis.

Another explanation for the acceptor-bound-exciton splitting was given by Ohkawa, Mitsuyu, and Yamazaki,<sup>77</sup> who suggest that the doublets they observe for  $I_1$  and  $I_2$  in N-doped MBE ZnSe are both due to strain splitting of the hole in the bound exciton. Their model for the  $I_1$  doublet is essentially a simplified and somewhat less accurate version of the one we present above, in which the hole-hole and crystal-field interactions are neglected.

#### IV. SUMMARY

A band-to-acceptor  $e-A^0$  transition in Li-doped  $p$ -type ZnSe grown by MBE has been clearly observed in low-temperature PL measurements. Measurements as a function of temperature and excitation level display the expected behavior for this type of transition and confirm the assignment. Allowing for the strain shift of the band gap, we obtain an accurate binding energy for Li acceptors of  $E_A^{\text{Li}} = 114.1$  meV in strained material, using the intercept of the  $e-A^0$  peak position plotted as a function of temperature. This technique of determining acceptor binding energies is found to be more accurate and reliable than rough estimates based on donor-acceptor pair peak positions or the use of Haynes's rule, which is not useful for accurate determinations of acceptor binding energies in ZnSe. It should be useful in determining accurate values of the binding energies of other shallow acceptors in ZnSe; such measurements are in progress. An anomalous initial quenching of the  $e-A^0$  peak intensity is ob-

served as the temperature is raised in the 1.7–15 K range, which is explained in terms of the temperature dependence of the competing nonradiative recombination rate. Above this temperature, normal behavior is observed. Magnetoluminescence measurements of the  $e-A^0$  peak display the expected linear shift with field and further support our assignment. By fitting the diamagnetic shift of the peak and neglecting apparently small spin splittings, we obtain an electron effective mass  $m_e^* = 0.17$ .

Our results clearly demonstrate that the 2.706-eV peak is not related to the  $R$  band previously observed in bulk material, which was an earlier identification of this peak. This conclusion demonstrates that there is no direct optical evidence for the presence of Li interstitial donors in this material. However, some type of compensating donor is clearly present to some degree, since significant donor-acceptor pair recombination is observed. Unfortunately, the PL measurements do not permit us to quantify this donor concentration. Attempts to identify the origin of these compensating donors will be reported elsewhere. The low-temperature PL properties of Li-doped ZnSe as a function of the Li-doping level and growth temperature have been shown and discussed. The  $e-A^0$  peak, which seems to occur only in some  $p$ -type-doped material, is frequently observed in  $p$ -type Li-doped samples grown under various conditions, and needs to be recognized whenever characterizing  $p$ -type ZnSe. A similar  $e-A^0$  peak has also been observed recently in N- and P-doped heteroepitaxial ZnSe grown by MBE,<sup>39</sup> indicating that it can occur for any acceptor species. We also identified an excited-state-donor-to-acceptor transition involving Li acceptors at high magnetic fields.

We observed two components of the Li acceptor-bound exciton in variable-temperature PL measurements of this strained heteroepitaxial material, whose positions are in agreement with several possible orderings of the neutral acceptor-bound exciton components at zero strain and their expected shifts and splittings under biaxial strain. Two sharp lines at 2.7421 and 2.7388 eV have been identified with the previously studied local-phonon-mode replicas of the Li-acceptor-bound-exciton peak, which confirms the incorporation of Li in this material. Finally, a series of discrete donor-to-acceptor pair lines is reported for the first time in Li-doped heteroepitaxial ZnSe.

#### ACKNOWLEDGMENT

The work at Arizona State University was supported by the National Science Foundation under Grant No. DMR-9106359.

<sup>1</sup>P. J. Dean and J. L. Merz, Phys. Rev. **178**, 1310 (1969).

<sup>2</sup>J. L. Merz, K. Nassau, and J. W. Shiever, Phys. Rev. B **8**, 1444 (1973).

<sup>3</sup>P. K. Chatterjee, A. J. Rosa, and B. G. Streetman, J. Lumin. **8**, 176 (1973).

<sup>4</sup>V. Swaminathan and L. C. Greene, Phys. Rev. B **14**, 5351

(1976).

<sup>5</sup>R. N. Bhargava, R. J. Seymour, B. J. Fitzpatrick, and S. P. Herko, Phys. Rev. B **20**, 2407 (1979).

<sup>6</sup>K. Kosai, B. J. Fitzpatrick, H. G. Grimmeiss, R. N. Bhargava, and G. F. Neumark, Appl. Phys. Lett. **35**, 194 (1979).

<sup>7</sup>G. F. Neumark, J. Appl. Phys. **51**, 3383 (1980).

- <sup>8</sup>G. F. Neumark and S. P. Herko, *J. Cryst. Growth* **59**, 189 (1982).
- <sup>9</sup>M. Ohishi, *Jpn. J. Appl. Phys.* **25**, 1546 (1986).
- <sup>10</sup>Yoichi Yamada, Isao Kidoguchi, Tsunemasa Taguchi, and Akio Hiraki, *Jpn. J. Appl. Phys.* **28**, L837 (1989).
- <sup>11</sup>M. Isshiki, K. S. Park, Y. Furukawa, and W. Uchida, *J. Cryst. Growth* **117**, 410 (1992).
- <sup>12</sup>H. Cheng, J. M. DePuydt, J. E. Potts, and T. L. Smith, *Appl. Phys. Lett.* **52**, 147 (1988).
- <sup>13</sup>J. M. DePuydt, M. A. Haase, H. Cheng, and J. E. Potts, *Appl. Phys. Lett.* **55**, 1103 (1989).
- <sup>14</sup>H. Cheng, J. M. DePuydt, J. E. Potts, and M. A. Haase, *J. Cryst. Growth* **95**, 512 (1989).
- <sup>15</sup>J. E. Potts, H. Cheng, J. M. DePuydt, and M. A. Haase, *J. Cryst. Growth* **101**, 425 (1990).
- <sup>16</sup>M. A. Haase, H. Cheng, J. M. DePuydt, and J. E. Potts, *J. Appl. Phys.* **67**, 448 (1990).
- <sup>17</sup>M. A. Haase, J. M. DePuydt, H. Cheng, and J. E. Potts, *Appl. Phys. Lett.* **58**, 1173 (1991).
- <sup>18</sup>T. Marshall and D. A. Cammack, *J. Appl. Phys.* **69**, 4149 (1991).
- <sup>19</sup>D. J. Olego, J. Petruzzello, T. Marshall, and D. Cammack, *Appl. Phys. Lett.* **59**, 961 (1991).
- <sup>20</sup>K. Hingerl, H. Sitter, J. Lilja, E. Kuusisto, K. Imai, M. Pessa, G. Kudlek, and J. Gutowski, *Semicond. Sci. Technol.* **6**, A72 (1991).
- <sup>21</sup>Z. Zhu, H. Mori, and M. Kawashima, *J. Cryst. Growth* **117**, 400 (1992).
- <sup>22</sup>K. Imai, E. Kuusisto, J. Lilja, M. Pessa, D. Suzuki, H. Ozaki, K. Kumazaki, and K. Hingerl, *J. Cryst. Growth* **117**, 406 (1992).
- <sup>23</sup>G. F. Neumark and S. P. Herko, *J. Cryst. Growth* **59**, 189 (1982).
- <sup>24</sup>P. J. Dean, H. Venghaus, and P. E. Simmonds, *Phys. Rev. B* **18**, 6813 (1978).
- <sup>25</sup>B. J. Skromme and G. E. Stillman, *Phys. Rev. B* **29**, 1982 (1984).
- <sup>26</sup>B. J. Skromme, R. Bhat, H. M. Cox, and E. Colas, *IEEE J. Quantum Electron.* **25**, 1035 (1989).
- <sup>27</sup>D. J. Robbins, P. J. Dean, P. E. Simmonds, and H. Tews, in *Deep Centers in Semiconductors*, edited by S. Pantelides (Gordon and Breach, New York, 1986), p. 717.
- <sup>28</sup>T. Kamiya and E. Wagner, *J. Appl. Phys.* **48**, 1928 (1977). See also corrections noted in Ref. 25.
- <sup>29</sup>S. Geczi and J. Woods, *J. Lumin.* **10**, 267 (1975).
- <sup>30</sup>G. Hitier, B. Canny, and J. F. Rommeluere, *J. Phys. (Paris)* **41**, 981 (1980).
- <sup>31</sup>D. M. Eagles, *J. Phys. Chem. Solids* **16**, 76 (1960).
- <sup>32</sup>R. Ulbrich, *Phys. Rev. B* **8**, 5719 (1973).
- <sup>33</sup>T. Yao, Y. Okada, S. Matsui, K. Ishida, and I. Fujimoto, *J. Cryst. Growth* **81**, 518 (1987).
- <sup>34</sup>B. J. Skromme, M. C. Tamargo, J. L. de Miguel, and R. E. Nahory, in *Epitaxy of Semiconductor Layered Structures*, edited by R. T. Tung, L. R. Dawson, and R. L. Gunshor, MRS Symposia Proceedings No. 102 (Materials Research Society, Pittsburgh, 1988), p. 577.
- <sup>35</sup>B. J. Skromme, M. C. Tamargo, F. S. Turco, S. M. Shibli, W. A. Bonner, and R. E. Nahory, in *Gallium Arsenide and Related Compounds*, edited by J. S. Harris (Institute of Physics, Bristol, 1989), p. 205.
- <sup>36</sup>P. J. Dean, D. C. Herbert, C. J. Werkhoven, B. J. Fitzpatrick, and R. N. Bhargava, *Phys. Rev. B* **23**, 4888 (1981).
- <sup>37</sup>D. Bimberg, *Phys. Rev. B* **18**, 1794 (1978).
- <sup>38</sup>B. J. Skromme, R. Bhat, M. A. Koza, S. A. Schwarz, T. S. Ravi, and D. M. Hwang, *Phys. Rev. Lett.* **65**, 2050 (1990).
- <sup>39</sup>Y. Zhang, B. J. Skromme, and H. Cheng (unpublished).
- <sup>40</sup>M. Schmidt, *Phys. Status Solidi B* **79**, 533 (1977).
- <sup>41</sup>H. Venghaus, *Phys. Rev. B* **19**, 3071 (1979).
- <sup>42</sup>D. J. Olego, T. Marshall, D. Cammack, K. Shahzad, and J. Petruzzello, *Appl. Phys. Lett.* **58**, 2654 (1991).
- <sup>43</sup>B. J. Skromme, M. C. Tamargo, J. L. de Miguel, and R. E. Nahory, *Appl. Phys. Lett.* **53**, 2217 (1988).
- <sup>44</sup>B. J. Skromme, M. C. Tamargo, F. S. Turco, S. M. Shibli, R. E. Nahory, and W. A. Bonner, in *Heteroepitaxial Approaches in Semiconductors: Lattice Mismatch and Its Consequences*, edited by A. T. Macrander and T. J. Drummond (Electrochemical Society, Pennington, NJ, 1989), Vol. 89-5, pp. 335-346.
- <sup>45</sup>J. R. Haynes, *Phys. Rev. Lett.* **4**, 361 (1960).
- <sup>46</sup>See, for example, P. J. Dean and D. C. Herbert, in *Excitons*, edited by K. Cho (Springer-Verlag, Berlin, 1979), p. 55, and references therein.
- <sup>47</sup>R. E. Halsted and M. Aven, *Phys. Rev. Lett.* **14**, 64 (1965).
- <sup>48</sup>P. J. Dean, W. Stutius, G. F. Neumark, B. J. Fitzpatrick, and R. N. Bhargava, *Phys. Rev. B* **27**, 2419 (1983).
- <sup>49</sup>R. N. Bhargava, *J. Cryst. Growth* **86**, 873 (1988).
- <sup>50</sup>H. Tews, H. Venghaus, and P. J. Dean, *Phys. Rev. B* **19**, 5178 (1979).
- <sup>51</sup>X. W. Fan and J. Woods, *IEEE Trans. Electron Devices* **ED-28**, 428 (1981).
- <sup>52</sup>A. Yoshikawa, S. Muto, S. Yamaga, and H. Kasai, *J. Cryst. Growth* **93**, 697 (1988).
- <sup>53</sup>J. A. Rossi, C. M. Wolfe, and J. O. Dimmock, *Phys. Rev. Lett.* **25**, 1614 (1970).
- <sup>54</sup>F. Willmann, W. Dreybrodt, M. Bettini, E. Bauser, and D. Bimberg, *Phys. Status Solidi B* **60**, 751 (1973).
- <sup>55</sup>W. Rühle and E. Göbel, *Phys. Status Solidi B* **78**, 311 (1976).
- <sup>56</sup>D. Bimberg and W. Rühle, *J. Phys. (Paris) Colloq.* **35**, C3-215 (1974).
- <sup>57</sup>D. Bimberg and W. Rühle, in *Proceedings of the 12th International Conference on the Physics of Semiconductors, Stuttgart, 1974*, edited by M. H. Pilkuhn (Teubner, Stuttgart, 1974), p. 561.
- <sup>58</sup>T. A. Kuhn, W. Ossau, A. Waag, R. N. Bicknell-Tassius, and G. Landwehr, *J. Cryst. Growth* **117**, 660 (1992).
- <sup>59</sup>J. L. Merz, H. Kukimoto, K. Nassau, and J. W. Shiever, *Phys. Rev. B* **6**, 545 (1972).
- <sup>60</sup>S. M. Huang, Y. Nozue, and K. Igaki, *Jpn. J. Appl. Phys.* **22**, L420 (1983).
- <sup>61</sup>T. Taguchi and T. Yao, *J. Appl. Phys.* **56**, 3002 (1984).
- <sup>62</sup>B. J. Skromme, N. G. Stoffel, A. S. Gozdz, M. C. Tamargo, and S. M. Shibli, in *Advances in Materials, Processing, and Devices for III-V Compound Semiconductors*, edited by D. K. Sadana, L. E. Eastman, and R. Dupuis, MRS Symposia Proceedings No. 144 (Materials Research Society, Pittsburgh, 1989), p. 391.
- <sup>63</sup>K. Shahzad, B. A. Khan, D. J. Olego, and D. A. Cammack, *Phys. Rev. B* **42**, 11 240 (1990).
- <sup>64</sup>Y. Zhang, B. J. Skromme, and F. S. Turco-Sandroff, *Phys. Rev. B* **46**, 3872 (1992).
- <sup>65</sup>E. U. Condon and G. H. Shortley, *The Theory of Atomic Spectra* (Cambridge University Press, Cambridge, 1977), Table 2<sup>10</sup>.
- <sup>66</sup>R. N. Bhargava, *J. Cryst. Growth* **59**, 15 (1982).
- <sup>67</sup>H. Mathieu, J. Camassel, and F. Ben Chekroun, *Phys. Rev. B* **29**, 3438 (1984).
- <sup>68</sup>P. J. Dean, B. J. Fitzpatrick, and R. N. Bhargava, *Phys. Rev. B* **26**, 2016 (1982).
- <sup>69</sup>G. Kudlek, N. Presser, J. Gutowski, D. R. Menke, M.

- Kobayashi, and R. L. Gunshor, in *Proceedings of the 20th International Conference on the Physics of Semiconductors*, edited by E. M. Anastassakis and J. D. Joannopoulos (World Scientific, Singapore, 1990), p. 1381.
- <sup>70</sup>J. Gutowski, N. Presser, and G. Kudlek, *Phys. Status Solidi A* **120**, 11 (1990).
- <sup>71</sup>G. Kudlek, N. Presser, J. Gutowski, K. Hingerl, H. Sitter, S. M. Durbin, D. R. Menke, M. Kobayashi, and R. L. Gunshor, *J. Appl. Phys.* **68**, 5630 (1990).
- <sup>72</sup>G. Kudlek, N. Presser, and J. Gutowski, *Semicond. Sci. Technol.* **6**, A83 (1991).
- <sup>73</sup>M. Schmidt, T. N. Morgan, and W. Schairer, *Phys. Rev. B* **11**, 5002 (1975).
- <sup>74</sup>C. Benoit á la Guillaume and P. Lavallard, *Phys. Rev. B* **5**, 4900 (1972).
- <sup>75</sup>P. J. Dean, M. J. Kane, N. Magnea, F. de Maigret, Le Si Dang, A. Nahmani, R. Romestain, and M. S. Skolnick, *J. Phys. C* **18**, 6185 (1985).
- <sup>76</sup>G. Kudlek, N. Presser, U. W. Pohl, J. Gutowski, J. Lilja, E. Kuusisto, K. Imai, M. Pessa, K. Hingerl, and H. Sitter, *J. Crys. Growth* **117**, 309 (1992).
- <sup>77</sup>K. Ohkawa, T. Mitsuyu, and O. Yamazaki, *Phys. Rev. B* **38**, 12465 (1988).